Dynamical features of a hydrogen-lithium complex in MgO:Li studied by EPR

V. M. Orera and M. L. Sanjuán
Instituto de Ciencia de Materiales de Aragón, Departamento de Optica, Universidad de Zaragoza, 50009 Zaragoza, Spain
(Received 29 July 1985)

H_i^0 (Li) defects in MgO undergo thermally activated reorientation motion at temperatures above 77 K. With the aid of the stochastic Liouville formalism we have studied the influence of such a motion on the EPR spectra. The contribution of both nonsecular and pseudosecular Hamiltonian terms to the averaging is discussed. It is shown that inclusion of pseudosecular terms in the simulation procedure is necessary in order to obtain agreement between the observed and the calculated spectra. Comparison between measured and simulated lines performed at different magnetic field orientations permits a precise determination of the jumping frequency ω_e as a function of temperature. The ω_e values follow an Arrhenius-type dependence on T with a barrier strength of 0.13 eV. Contributions to the line shapes from partially unresolved superhyperfine interactions are also discussed.

I. INTRODUCTION

The hydrogen impurity almost always present in binary oxides greatly modifies some properties of the binary oxides. For this reason in the last few years a big effort has been focused on studying hydrogen and hydrogen-related centers in these compounds.[1-3] In spite of these efforts information about well-established models for such defects in oxides is still lacking.

Recently, the production by liquid-nitrogen-temperature (LNT) irradiation of a hydrogen-lithium mixed defect in MgO:Li crystals has been reported.[4] The EPR spectrum, thermal stability, and bleaching behavior indicate that the center consists of an interstitial atomic hydrogen close to a substitutional Li^+ ion. Similar configurations have been detected in alkali halides.[5] The absence of well-resolved superhyperfine interactions, other than with the lithium ion, prevents a precise determination by EPR of the positions of the ions; in consequence, the molecular character of the center cannot be decided. In the following we will describe this defect as a perturbed interstitial hydrogen center H_i^0(Li).

An interesting feature of H_i^0(Li) defects is that they reorient at temperatures above 77 K.[4] The study of the dynamical properties of defects in solids permits the determination of some characteristic motion-related parameters such as hopping rates and activation energies which are useful to check the defect models.

The magnetic resonance technique is appropriate to study the reorientation of H_i^0(Li) defects because they are paramagnetic species with anisotropic spin-Hamiltonian parameters. Dynamical effects in the magnetic resonance are studied by introduction of time-dependent spin-Hamiltonian terms into the spin-dynamical equations. The time-dependent terms describe the coupling of the spin system to the lattice either through lattice vibrations or defect motions. For defect motion, long correlation times are expected, and general relaxation theories[6] are not applicable over the entire range. On the other hand, adiabatic theories provide a way of studying the process from the static to the fast-motion region,[7] but they require that the anisotropic components be small. That is not the case for H_i^0(Li) defects in MgO.

The theory we have applied here uses the stochastic Liouville method with the assumption of a Markovian process for the motion. That theory has been extensively used to study molecular motion in liquids, organic crystals, and liquid crystals.[8,9] Only recently has it been applied to defect motions in fluorites[10] and oxides.[11] Using this theory the EPR spectra are calculated for different values of the hopping rates. In the solid state, spectra taken at the same temperature (i.e., the same hopping rate), but with different magnetic field orientations present signals at different stages of averaging. This fact enables a precise determination of the motion parameters in spite of the presence of unresolved contributions to the line shapes arising from interactions with lattice ions and other defects which complicate the simulation procedure. The influence of pseudosecular Hamiltonian components in the calculations is also discussed. Inclusion of these terms enables us to account even for some minor details of the experimental spectra. Finally, the hopping rates are given as a function of temperature. The results fit an Arrhenius-type law indicating that the hopping process can be interpreted as due to thermally activated jumps over a barrier.

II. EXPERIMENTAL

MgO single crystals doped with 0.03—0.05 at. % Li were grown at Oak Ridge National Laboratory by the arc-fusion technique using MgO powder of the Kanto Chemical Company, mixed with Li_2CO_3.[12] Other impurities such as Mn, Cr, and Fe which produce paramagnetic defects were also present.

EPR measurements were taken in a Varian E-112 spectrometer working in the X band. A Varian E-257 continuous-flow cryostat was used for measurements between LNT and room temperature. The temperature was measured with a ± 2 K precision.

III. EXPERIMENTAL RESULTS

The EPR spectrum of $H_i^0(Li)$ centers taken at LNT has been studied previously by Orera *et al.*[4] The spectrum consists of two groups of lines about 450 G apart. This splitting is due to the hyperfine (hf) interaction of the unpaired electron with the proton. Each group presents the structure due to the superhyperfine interaction (shf) with lithium. The defect has a trigonal symmetry.

At temperatures above LNT, the EPR pattern is strongly modified. We describe in the following the evolution of the spectra with temperature taking as an example the EPR measurements with the external magnetic field H_0 along either the ⟨100⟩ or the ⟨110⟩ directions.

In Fig. 1 we plot the spectra corresponding to the high-field group of lines measured with $H_0||[100]$ at temperatures between 77 K and the upper stability limit of $H_i^0(Li)$ defects ($\sim$200 K). At LNT the spectrum consists of four equidistant lines ($\sim$9 G apart) due to the shf interaction with the 92.58%-abundant ^7Li isotope ($I=\frac{3}{2}$). Three weak lines in the central part of the spectrum are assigned to the interaction with the 7.42%-abundant ^6Li ($I=1$).

It is interesting to point out that all the EPR spectra have been taken at very low microwave power levels ($\lesssim$0.02 mW). At higher levels the main lines saturate and other signals appear (as can be seen in Fig. 1 of Ref. 4). Some of them correspond to "forbidden" transitions (as indicated in the computer simulations explained in the next sections) whose positions are given in the figure by crosses. The others are of unknown origin.

As the temperature increases the lines broaden and move. The broadening is not uniform; the outer lines are narrower than the inner ones. There is also a slight displacement of the group as a whole towards low fields together with a decrease in the shf splitting. At the same time the forbidden lines disappear. Above 145 K the lines start to narrow [Fig. 1(c)] and finally all the lines reach the same intensity. The narrowing effect appears in the ^6Li shf spectrum at lower temperatures than in the ^7Li spectrum. As the lines narrow some weak lines emerge from each individual shf line.

When the magnetic field is away from the [100] direction a different behavior is observed. In Fig. 2 we give the evolution with temperature of the high-field group of lines measured with $H_0||[110]$. At LNT the spectrum consists of two groups of four lines each (for ^7Li isotope) corresponding to the two inequivalent orientations of the centers with respect to the magnetic field. Due to the anisotropy of both hydrogen and lithium hf interactions, the splitting of each lithium shf component into the two lines

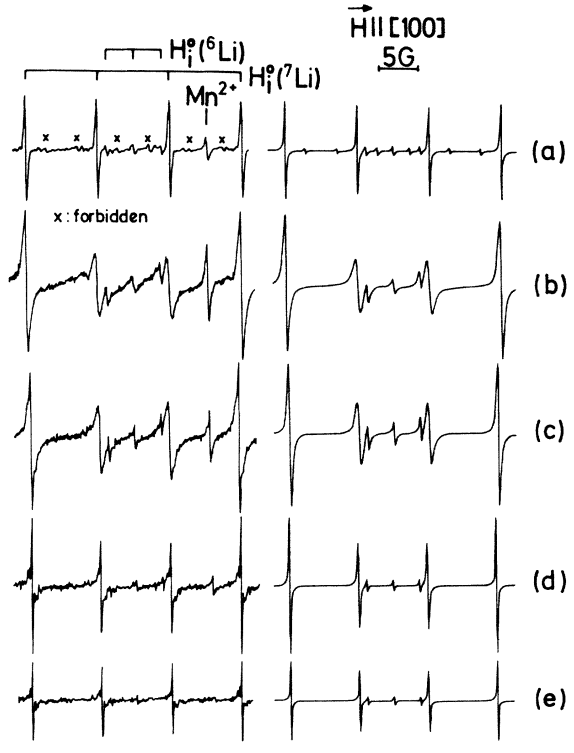

FIG. 1. Temperature evolution of the EPR spectrum with $H_0||[100]$ (left) and computer simulation for each temperature (right). The intensity gain G is different for each spectrum. (a) $T=77$ K, $\omega_e\simeq 0$ MHz; (b) $T=129$ K, $\omega_e=3.15$ MHz; (c) $T=162$ K, $\omega_e=31.5$ MHz; (d) $T=192$ K, $\omega_e=150$ MHz; (e) $T=211$ K, $\omega_e=300$ MHz.

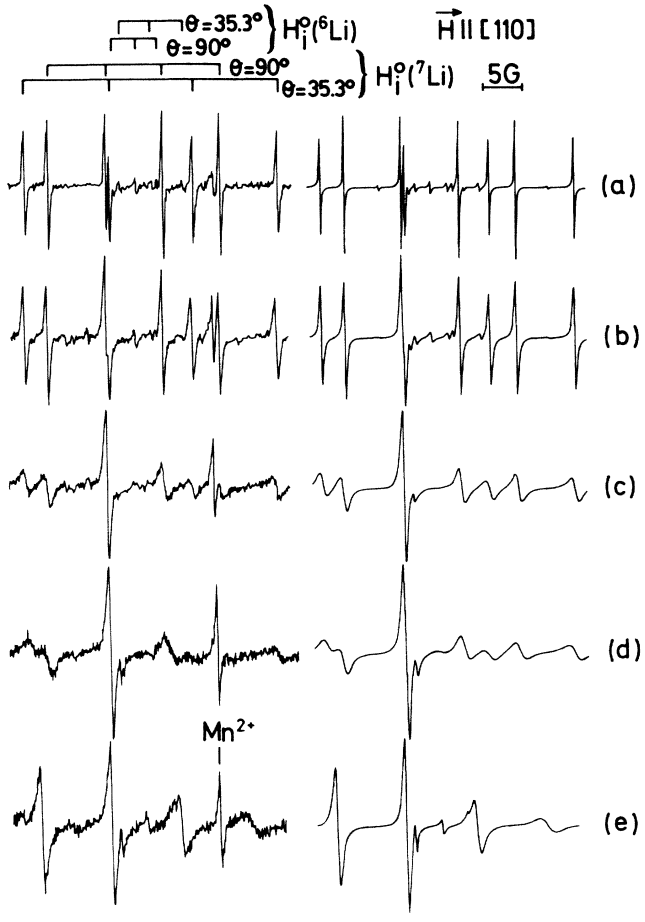

FIG. 2. Temperature evolution of the spectra with $H_0||[110]$ (left) and computer simulations (right). (a) $T=77$ K, $\omega_e\simeq 0$ MHz; (b) $T=112$ K, $\omega_e=0.45$ MHz; (c) $T=126$ K, $\omega_e=2.4$ MHz; (d) $T=132.5$, $\omega_e=3.9$ MHz; (e) $T=156.5$ K, $\omega_e=22.5$ MHz.

is not uniform. The same fact is observed in the two groups of three lines due to the shf interaction with ^{6}Li nuclei. The position of the static lines is given at the top of the figure by sticks.

As the temperature is increased, the lines broaden and move. Besides the overall small shift on the high-field group towards lower fields, each pair of lines tend to coalesce into a single line. The rate of coalescence depends on the initial splitting. This is illustrated in Fig. 3, where we show the evolution of the shifts between pairs of lines corresponding to the two inequivalent sets of centers when $\mathbf{H}||[110]$ as a function of temperature. Once the averaging is completed each line begins to narrow; at the same time some weak signals emerge from each single line.

IV. LINE-SHAPE THEORY

In order to simulate the EPR spectrum over all of the measured temperature range and for all magnetic field orientations we will use a theory based on the stochastic Liouville formalism, which is valid from the static through the motional narrowing region.

The theory starts from the dynamical equation for the total density matrix of the system, $\rho(t)$

$$i\frac{d\rho(t)}{dt}=[\mathscr{H}(t),\rho(t)] \ , \tag{1}$$

where $\mathscr{H}(t)$ is the time-dependent Hamiltonian that can be written as

$$\mathscr{H}(t)=\mathscr{H}_S+\mathscr{H}_L+\mathscr{H}_{SL}+\epsilon(t) \ , \tag{2}$$

with $\mathscr{H}_S$ the spin Hamiltonian of the defect, which in our case is anisotropic, $\mathscr{H}_L$ the lattice Hamiltonian, $\mathscr{H}_{SL}$ the spin-lattice interaction, and $\epsilon(t)$ the interaction with the microwave field.

Averaging over the lattice degrees of freedom[13,14] leads to the stochastic equation for the time evolution of the reduced density matrix $\rho'(t)$

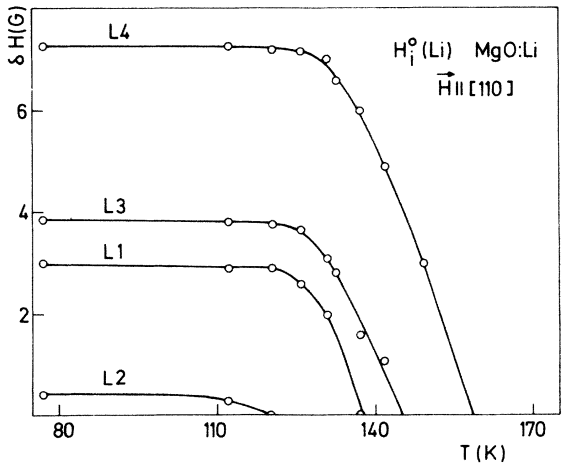

FIG. 3. Temperature evolution of the anisotropic splitting of each lithium hf component when $\mathbf{H}_0||[110]$. Experimental (open circles) and calculated (solid line) values. The four lithium hf lines are labeled $L1$, $L2$, $L3$, and $L4$ from low- to high-field positions, respectively.

$$i\frac{d\rho'(t)}{dt}=[\mathscr{H}_S+\epsilon(t),\rho'(t)] \\ -i\tilde{\Gamma}[\rho'(t)-\rho_{eq}]-i\tilde{R}[\rho'(t)-\rho_{eq}] \ , \tag{3}$$

with $\rho'(t)$ a function of both spin and orientation coordinates of the defect. The jumping process is assumed to be of stationary Markovian character. Then $\tilde{\Gamma}$ is a Markovian evolution operator which accounts for that part of the spin-lattice interaction causing the defect motion.[15]

The random fluctuations due to lattice vibrations have a characteristic correlation time much shorter than that for defect reorientation. In that case the two effects can be treated separately[16] and the usual spin relaxation is introduced into the dynamical equation through the relaxation matrix $\tilde{R}$. The equilibrium density ρ_{eq} is added in order to ensure that the system relaxes to thermal equilibrium.

Using the fact that the anisotropic contribution to $\mathscr{H}_S$ is small compared with the isotropic part $\mathscr{H}_0$ we can write

$$\rho_{eq}=\frac{1}{Z}\exp(-\mathscr{H}_o/kT) \ ,$$

where Z is the partition function of the system. The approximation implies equal distribution probabilities at different sites and an isotropic jump frequency. In the high-temperature approach

$$\rho_{eq}\simeq\frac{1}{Z}-\frac{\mathscr{H}_0}{kTZ} \ .$$

In order to calculate the spectrum, the matrix elements of the operators involved in Eq. (4) are taken in the basis $|\sigma j\rangle$, where σ stands for the electronic and nuclear-spin quantum numbers and j for the different orientations of the defect. In the extended superspace $\tilde{\Gamma}$ produces the coupling between states having the same spin quantum numbers and different orientations. The matrix element $\tilde{\Gamma}_{jk}$ is defined as the probability per unit time of jumping from site j to site k.

H_i^0(Li) centers present eight crystallographically equivalent orientations. In consequence an eight-dimensional orientation space is needed to describe the motion. Due to inversion symmetry of the magnetic interactions, jumps between opposite sites (180°) do not contribute to the averaging. This allows us to reduce that dimension to four. Hopping motion between either nearest-neighbor sites (70.5°) or next-nearest-neighbor sites (109.5°) leads to the same reduced transition matrix $\tilde{\Gamma}$ which is found by

$$\Gamma_{ij}=-\omega_e x\begin{cases}-1 \text{ if } i=j \ , \\ \frac{1}{3} \text{ if } i\neq j \ ,\end{cases} \tag{4}$$

where ω_e is the total probability per unit time of jumping from one site to any other. In case that both types of jumps are included at the same time with different jump probabilities, the matrix $\tilde{\Gamma}$ will be the same but then ω_e will be the sum of the two frequencies.

Finally, the relaxation matrix $\tilde{R}$ is introduced in diagonal form with an adjustable parameter γ which stands for

the linewidth in the absence of motion.

Equation (3) operates over the extended superspace of spin and orientation variables. Experiments were performed with microwave powers low enough to avoid saturation. In that case the problem reduces to solving a set of $n^2 s$ linear-dependent equations (n is the dimension of spin space and s that of the orientation space). This can be done by means of a computer, and the solution is introduced into the EPR absorption spectrum, which is given by

$$I(\omega) \propto \mathrm{tr}(S_+ \{ \mathrm{Im}[Z^1(\omega)] \}) \ , \tag{5}$$

where the trace is over both spin and orientations coordinates and $Z^1(\omega)$ is the Fourier transform of $\rho'(t) - \rho_{\mathrm{eq}}$.

V. INTERPRETATION AND DISCUSSION

The EPR spectrum of $H_i^0(\mathrm{Li})$ centers in the static limit (below 80 K) was explained using the spin Hamiltonian

$$\mathcal{H}_S = \mu_B g \mathbf{H}_0 \cdot \mathbf{S} + a \mathbf{I}^{\mathrm{H}} \cdot \mathbf{S} + b(3 I_z^{\mathrm{H}} S_z - \mathbf{I}^{\mathrm{H}} \cdot \mathbf{S}) + A_\perp (S_x I_x^{\mathrm{Li}} + S_y I_y^{\mathrm{Li}}) + A_{||} S_z I_z^{\mathrm{Li}} \ , \tag{6}$$

with the z axis along a $\langle 111 \rangle$ direction and with the following parameters: $g = 2.002 \pm 0.001$, $a = 1240 \pm 10$ MHz, $b = 5.6 \pm 0.2$ MHz, $A_{||} = 33.3 \pm 0.2$ MHz, and $A_\perp = 20.1 \pm 0.2$ MHz.

Addition of the Li Zeeman nuclear term $-\mu_N g_N \mathbf{I}^{\mathrm{Li}} \cdot \mathbf{H}_0$ to Eq. (6) enables us to account for the weak doublets appearing between the Li shf lines. In fact these lines are "forbidden" in the sense that they involve flipping of both electron and nuclear spins. The forbidden line pattern depends strongly on the choice of the relative signs of $A_{||}$ and $A_\perp$. The experimental results yield $A_{||}/A_\perp > 0$.

The ^{6}Li hyperfine spectrum corresponds, as expected, to values of the hyperfine constants given by

$$\frac{A(^6\mathrm{Li})}{A(^7\mathrm{Li})} = \frac{g_N(^6\mathrm{Li})}{g_N(^7\mathrm{Li})} = 0.38 \ .$$

When the temperature increases some changes take place in the EPR spectra, which can be interpreted as due to the effect of hopping motion of the defects among the eight crystallographically equivalent orientations.

Usually, two types of formalism have been used to explain the averaging processes. Approximative ones (such as the adiabatic theory or the secular approximation, both leading to modified Bloch equations[17]) predict, when they are applicable, the main features of the averaging and enable one, through rather simple relationships, to obtain the temperature dependence of the jump frequency.

In our case, and because of the anisotropy of the hyperfine interactions no basis can be found in which the spin Hamiltonians of the eight possible configurations are diagonal at once. The spin operators involved in $\mathcal{H}_S$ that do not commute with $\mathcal{H}_0$ lead to pseudosecular terms, producing nuclear spin flips, and nonsecular terms, which induce electron-spin transitions. The density-matrix formalism admits, in a natural way, the inclusion of those nondiagonal Hamiltonian terms responsible for the nonadiabatic effects.

The calculation procedure has been outlined in Sec. IV. The problem reduces to solve a set of 1024 (256×4) linear-dependent equations. The dimension is prohibitively large and a reduction is required. A first reduction can be achieved if one uses the basis of eigenstates of $\mathcal{H}_0$ (electron Zeeman term plus isotropic part of the hydrogen hf interaction). Neglecting nonsecular terms in the rest of the hydrogen hf contribution the high- and low-field groups of lines can be handled separately. A further reduction is obtained by also neglecting nonsecular terms in the lithium interactions. The final dimension is 64.

The influence of the approximations mentioned above has been checked by means of two-site jump simulations. It is proved that the neglected nonsecular terms do not meaningfully contribute to the spectra. On the contrary, pseudosecular terms have important effects in the averaging process.

As an example let us discuss which are the changes with ω_e in the $\mathbf{H}_0 || [100]$ spectra. In the static limit the spectrum consists of four lines equally spaced by

$$a_{\mathrm{eff}}[100] = (A_{||}^2/3 + 2A_\perp^2/3)^{1/2}$$

(high-field approximation). Adiabatic theories or secular approximations, which neglect the effect of pseudosecular terms in the averaging, predict no changes with ω_e either in the splitting or in the half-widths or relative intensities of the lines.[18]

The experiments show a change in the lithium hyperfine splitting from the static to the averaged case of -0.35 G. The inclusion of pseudosecular terms within the framework of density-matrix stochastic theory accounts for this effect which corresponds to an averaging of the shf splitting from $a_{\mathrm{eff}}[100]$ (for $\omega_e = 0$) to $a_{\mathrm{av}} = \frac{1}{3}(A_{||} + 2A_\perp)$ (for $\omega_e \to \infty$). This effect also occurs in the hydrogen hf splitting but, due to the small anisotropy of this interaction it is almost negligible and cannot account for the observed shift of the hyperfine splitting with T. This dependence is close to linear ($\sim -1 \times 10^{-3}$ mT K^{-1}) and must be explained by a change of the isotropic parameter with T. Its influence on the simulated spectra is negligible except for the position of the lines and has been taken into account.[19]

Pseudosecular terms also produce motion-induced changes with ω_e in the half-widths and relative intensities of the lines as observed in the experimental spectrum. It is interesting to point out that contrary to the static parameter a_{eff} the averaged one is sensitive to the choice of the relative signs of $A_{||}$ and $A_\perp$. The experiments lead to $A_{||}/A_\perp > 0$ in agreement with the previous relation obtained from the "forbidden" lines pattern. When the spectra are measured with $\mathbf{H}_0 || [110]$ the influence of pseudosecular terms is partially masked by the stronger secular effects although their contribution is still important if quantitative agreement is wanted.

Using the formalism described in Sec. IV and the spin Hamiltonian Eq. (6) together with the approximations mentioned above we have simulated the $H_i^0(\mathrm{Li})$ EPR spectra. Two temperature-dependent unknown parameters ω_e and γ enter our calculations. Three magnitudes (line position, intensity, and linewidth) have been used to characterize our spectra. Depending on the stage of averaging each of them is more or less sensitive to the unknown parame-

ters. Specifically for hopping-rate determinations, the line position is the best observable when ω_e is smaller than the anisotropy to be averaged out. As ω_e increases the lines reach their "isotropic" averaged position. The intensities and/or the half-widths are then the useful observables.

In our case, the splittings between shf lines when $\mathbf{H}_0 \| [110]$ are the best experimental observables to fit. Due to the differences in the initial splittings, the averaging stages of each doublet at a given temperature are also different. Simultaneous fitting of all the splittings leads to a precise determination of ω_e as a function of T. This procedure is valid up to values of $\omega_e \simeq 20$ MHz. Comparison between the experimental and calculated line positions is given in Fig. 3.

A difficulty arises when besides the line positions we also want to fit the line shapes in this ω_e value range. In fact, in order to account for the observed intensities and linewidths a temperature- and line-dependent intrinsic linewidth parameter γ has to be introduced into the calculations. Moreover the calculated lines are essentially Lorentzians, while the observed ones are more Gaussian. This situation is rather general in the studies performed in the solid state[10,11] and it has been attributed to the presence of unresolved interactions with other ions and defects causing the observed inhomogeneous broadening of the lines.

In our case the explanation for this behavior is clear. In the extreme narrowed region a pattern of several weak lines is observed at both sides of each individual line. This pattern can be interpreted as due to the shf interaction of the electronic spin with the 10.13%-abundant nearest-neighbor ^{25}Mg isotopes ($I = \frac{5}{2}$). Near the rigid limit the shf pattern should consist of several weak lines, due to the interaction with one, two or three nearest ^{25}Mg atoms, at both sides of each central one (corresponding to defects whose three Mg neighbors have $I = 0$). Due to the small relative probability of having ^{25}Mg isotopes close to the defect this pattern is scarcely observed at LNT. As temperature increases the defect starts to jump between the eight crystallographically equivalent positions. As a consequence of the motion the defect interacts with twelve nearest Mg ions instead of three. The relative probabilities of having close ^{25}Mg atoms increase and some shf lines emerge at the expense of the central one. At the same time the lines broaden. Due to all these phenomena the ^{25}Mg shf interactions become unresolved causing the observed distortions in the lineshapes.

In the narrowed stage the shf interaction is again almost completely resolved and the central line can be fitted with a temperature-independent parameter γ similar to the static one. Consequently, the half-widths and/or the intensities of the lines are good observables in order to get accurate ω_e values in this region. The narrowed stage is reached at lower temperatures when $\mathbf{H}_0 \| [100]$ than for other magnetic field orientations. We have used these spectra to obtain the hopping rates above 150 K.

The explanation given above for the effect of the ^{25}Mg shf interaction on the averaged spectra has been discussed in a qualitative way. A direct inclusion of this interaction in the calculations is cumbersome. More elaborated approximations are necessary which will be presented in a separate paper.

In Figs. 1 and 2 we present some examples of the procedure strength. It can be seen that the calculated spectra account for most of the details of the experimental ones. The study of the temperature dependence of the jump frequency gives information about the mechanisms involved in the defect reorientation. The low intensity-to-noise ratio of the ^{6}Li shf pattern prevents us from detecting any isotopic effect on the jump rates. In Fig. 4 we give a plot of ω_e versus T^{-1}. The data fit the exponential law given by

$$\omega_e = \omega_0 \exp(-E_a/kT) \ ,$$

where ω_0 is the infinite temperature frequency and E_a is the barrier strength with $\omega_0 \simeq 4 \times 10^{11}$ Hz and $E_a = 0.13(1)$ eV. This result indicates that the mechanism of H_i^0(Li) defect reorientation can be explained by thermally activated jumps over the potential barrier between equivalent sites.

As we have already said, the symmetry of the defect prevents us from distinguishing between 70.5° and 109.5° jumps. Besides that, if the two types of jumps coexist, the simulation procedure would lead to ω_e values which are the sum of the two jump frequencies. On the other hand, different barrier strengths can be expected for both types of jumps. Since ω_e depends on T exponentially, the addition of two exponential functions should give a departure of the total ω_e from a single exponential dependence, which has not been observed.

We conclude that both types of jumps do not coexist in the measured temperature range. Taking into account the packing of atoms on the MgO planes it seems that jumps of an interstitial hydrogen along the ⟨100⟩ directions (70.5° jumps) are the most probable.

The establishment of a precise model for H_i^0(Li) center

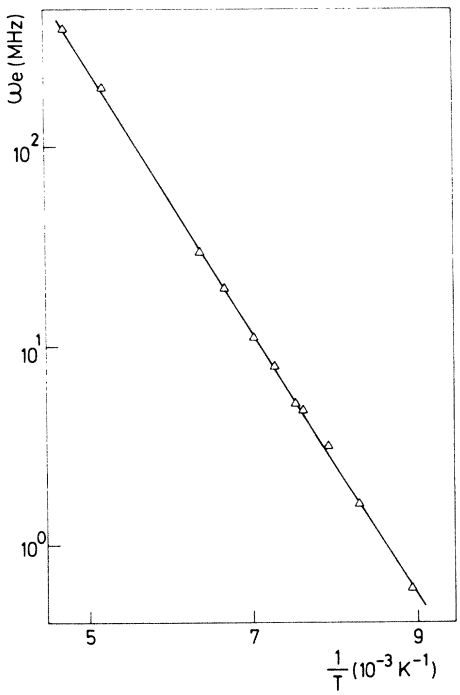

FIG. 4. Semilogarithmic plot of the jump frequency ω_e vs $1/T$.

and its dynamic behavior requires a thorough analysis of the shf interactions. Electron-nuclear double resonance measurements and studies of the high-temperature resolved ^{25}Mg interactions are under way.

ACKNOWLEDGMENT

We wish to thank Dr. Y. Chen of Oak Ridge National Laboratory for providing us with the MgO:Li samples.

[1]R. González, Y. Chen, and K. L. Tsang, Phys. Rev. B **26**, 4637 (1982).
[2]B. T. Jeffries, R. González, Y. Chen, and G. P. Summers, Phys. Rev. B **25**, 2077 (1982).
[3]Y. Chen, R. González, O. E. Schow, and G. P. Summers, Phys. Rev. B **27**, 1276 (1983).
[4]V. M. Orera, P. J. Alonso, and R. Alcalá, J. Phys. C **16**, 783 (1983).
[5]G. Heder and J. M. Spaeth, Phys. Status. Solidi. B **125**, 523 (1984).
[6]C. P. Slichter, *Principles of Magnetic Resonance* (Springer-Verlag, Berlin, 1978).
[7]C. S. Johnson, Advan. Mag. Res. **1**, 33 (1965).
[8]J. H. Freed, G. V. Bruno, and C. F. Polnaszek, J. Phys. Chem. **75**, 3385 (1971).
[9]C. F. Polnaszek, G. V. Bruno, and J. H. Freed, J. Chem. Phys. **58**, 3185 (1973).
[10]H. Bill, J. Chem. Phys. **70**, 277 (1979); **76**, 219 (1982).
[11]M. L. Sanjuán, and V. M. Orera, J. Phys. C (to be published).
[12]M. M. Abraham, C. T. Butler, and Y. Chen, J. Chem. Phys. **55**, 3752 (1971).
[13]J. Bretón, A. Hardisson, F. Mauricio, and S. Velasco, Phys. Rev. A **30**, 542 (1984).
[14]R. M. Lynden-Bell, Mol. Phys. **22**, 837 (1971).
[15]W. Peier, Physica **57**, 565 (1972).
[16]J. Jeener, Adv. Mag. Res. **10**, 1 (1982).
[17]J. H. Freed, Ann. Rev. Phys. Chem. **23**, 265 (1972).
[18]In the first case, the static spectrum is well reproduced but not the averaged one. The secular approximation leads to four lines shifted by a_{av}, so it reproduces the averaged spectrum (but not the static one). Neither of them are valid at an intermediate stage of averaging.
[19]Presumably proportional changes with T exist in the lithium shf constants but they are not observed due to the small value of these constants as compared with the hydrogen ones.